References

[1] Steg, L. and Lew, H. G., "Hypersonic ablation," AGARD Hypersonic Conference, TCEA Rhode-St. Genese, Belgium (April 3–6, 1962); also General Electric Co., Missile and Space Div., TIS-R62SD55 (May 1962).

[2] Hurwicz, H., "Aerothermochemistry studies in ablation," Fifth AGARD Combustion and Propulsion Colloquium, Brunswick, Germany (April 9–13, 1962).

[3] Schmidt, D. E., "Ablation of plastics," Aeronautical Systems Div. TR-61-650 (February 1962).

[4] Buhler, R. D., Christensen, D., and Grindle, S., "Effects of hyperthermal conditions on plastic ablation materials," Aeronautical Systems Div. TR-61-304, Plasmadyne Corp., (January 1962).

[5] Mixer, R. Y. and Marynowski, C. W., "A study of the mechanism of ablation of reinforced plastics," Wright Air Development Center TR 59-668, Part I (February 1960).

[6] Barry, W. T. and Sutton, W. H., "The importance of char structures in the ablation performance of organic polymers," General Electric Co., Missile and Space Div., TIS-R60SD329 (March 11, 1960).

[7] Robbins, D. L., "Thermal erosion of ablative materials," Aeronautical Systems Div. TR-61-307, Aerojet-General Corp. (April 1962).

[8] Barry, W. T. and Gaulin, C. A., "A study of physical and chemical processess accompanying ablation of G.E. century resins," General Electric Co., Missile and Space Div., TIS-R62SD2 (May 1962).

[9] Schmidt, D. L., "Behavior of plastic materials in hyperthermal environments," Wright Air Development Center TR 59-574 (April 1960).

[10] Myers, H. and Harmon, D., Jr., "Energy transfer processes in decomposing polymeric systems," Engineering Paper 1020, Missile and Space Systems Engineering, Douglas Aircraft Co. (September 1960).

[11] Vojvodich, N. S. and Pope, R. B., "Effect of gas composition on the ablation behavior of a charring material," AIAA J. **2**, 536–542 (1964).

[12] Dhanak, A. M., "A theoretical study of mechanical erosion from a charred surface in boundary layer flows," AVCO RAD-7-TM-60-74 (December 1960).

[13] Scala, S. M. and Gilbert, L. M., "Thermal degradation of a char-forming plastic during hypersonic flight," ARS J. **32**, 917–924 (1962).

[14] Mathieu, R. D., "Response of charring ablators to hyperthermal environment," General Electric Co., Missile and Space Div., TIS-R63SD20 (February 1963).

[15] Munson, T. A. and Spindler, R. J., "Transient thermal behavior of decomposing materials, Part I, General theory and application to convective heating," IAS Paper 62-30 (January 1962).

[16] Friedman, H. L., "The pyrolysis of plastics in a high vacuum arc image furance," General Electric Co., Missile and Space Div., TIS-R62SD57 (December 1962).

[17] Friedman, H. L., "The kinetics of thermal degradation of charring plastics," General Electric Co., Missile and Space Div., TIS-R61SD145 (August 1961).

[18] Tavakoli, M. L., private communication (November 1961).

[19] Swann, R. T. and Pittman, C. M., "Numerical analysis of the transient thermal response of advanced thermal protection systems for atmospheric entry," NASA TN D-1370 (July 1962).

[20] Menkes, E. G., "Analysis of the structural behavior of charring ablator heat protection systems," General Electric Co., Missile and Space Div. (to be published).

SEPTEMBER 1964 AIAA JOURNAL VOL. 2, NO. 9

Time for a Totally Wetting Liquid to Deform from a Gravity-Dominated to a Nulled-Gravity Equilibrium State

HOWARD L. PAYNTER*
Martin Company, Denver, Colo.

This article presents an analytical method to predict the time required for a liquid/vapor system to deform from a gravity-dominated condition to that of a nulled-gravity equilibrium state. The theoretical analysis assumes that the free surface is completely transformed to kinetic energy during this deformation. The physical model is a spherical container partially filled with a totally wetting liquid. A dimensionless coefficient, a function of tank radius only, was then employed to modify the theoretical analysis and to provide good correlation between analytical results and NASA experimental data.

Nomenclature

SE = surface energy, ft-lbf
KE = kinetic energy, ft-lbf
H = correlation coefficient
σ = surface tension, lbf/ft
R, r = radius, ft or cm
R_c = constant, 1 cm
v = velocity, fps
m = mass, lbm
ρ = mass density, lbm/ft^3
τ_p = zero-g elapsed time parameter, dimensionless
τ = time, sec
g_c = 32.174 lbm-ft/lbf-sec^2
V = volume, ft^3
K = Harkins' spreading coefficient
ξ = ratio, liquid-to-container volume
β = kinematic surface tension, ft^3/sec^2

Subscripts

l = liquid
n = refers to the nth increment ($1 \leq n \leq 30$)
lv = liquid/vapor
sv = solid/vapor
sl = solid/liquid
0 = initial

Received October 21, 1963; revision received May 18, 1964.

* Design Specialist, Advanced Development and Technology Section, Propulsion and Mechanical Engineering Department. Member AIAA.

Introduction

ZERO-GRAVITY, and associated fluid problems, are discussed in Refs. 1–4. A particular problem for the designer of liquid rocket engines is predicting the time required

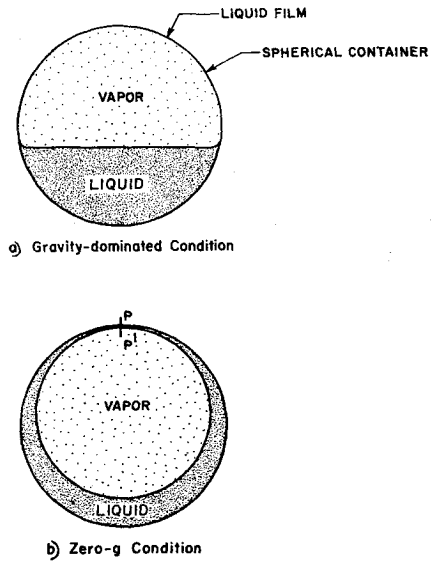

Fig. 1 Fluid system equilibrium.

for a subcritically stored propellant, i.e., liquid and vapor, to deform from a gravity-dominated state to a weightless equilibrium condition.

NASA presents drop-test data for a totally wetting liquid, ethyl alcohol, to reach a minimum surface energy condition.[5] These data do not represent the time for zero-g equilibrium to be reached, since the liquid possesses finite kinetic energy when minimum surface energy is first attained. This is shown in Fig. 1. The gravity-dominated condition is pictured in Figure 1a. The bulk of the liquid is gravity-oriented with a thin liquid film covering the container surface not in direct contact with the liquid bulk. This liquid film, caused by extremely small surface tension forces, is affected by gravity in thickness only due to inertia. Under a gravity condition, this film may be but a few molecules thick; whereas, when the effect of gravity is nullified (as in Fig. 1b), this thickness can be appreciable.

The initial minimum surface energy condition in zero-g is shown in Fig. 1b. The liquid-vapor interfacial area is at a minimum. The system has deformed from its gravity-dominated state to entrap the spherical vapor bubble. However, when this initial condition is attained, the liquid meets at station $P - P^1$ with a finite kinetic energy. The NASA data show this phenomenon. Eventually this energy is dissipated by doing work on the embedded vapor and in viscous shear of the liquid. This energy dissipation process is not considered in this analysis. Zero-g equilibrium, as used in this treatise, denotes the condition when minimum surface energy for the two-phase fluid system is first attained (Fig. 1b).

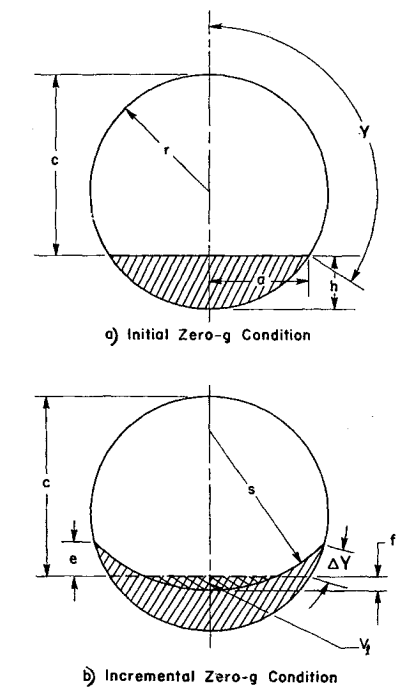

Fig. 2 Incremental zero-g energy change.

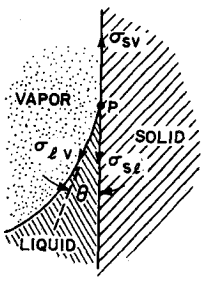

Fig. 3 Intermolecular force diagram.

This analytical method of estimating the elapsed time in zero-g for liquid to reach equilibrium is of particular significance to the designer of liquid rocket engines since most propellants, such as nitrogen tetroxide, Aerozene "50," and the cryogenics, are totally wetting.

Discussion

Assumptions

The following assumptions were used in the analysis.

1) Free surface energy is completely transformed to liquid kinetic energy during the liquid/vapor deformation process. The gravity-dominated and zero-g equilibrium conditions are shown in Fig. 1, and incremental fluid deformation in attaining Fig. 1b is presented in Fig. 2.

2) Heat and viscosity effects are negligible.

3) Bond number (dimensionless ratio of gravity-to-capillary forces) is zero, i.e., gravity forces are completely nullified.

4) The liquid/vapor interface (s in Fig. 2) is of constant curvature.

5) The displaced liquid volume V_l in Fig. 2 is the only liquid accelerated during deformation.

6) The initial zero-g liquid/vapor system condition, or gravity-dominated state, is as in Fig. 1a. A thin liquid layer covers the entire wall surface not in contact with the liquid glob.

Assumption 5 can be a first approximation only since the exact liquid mass accelerated during the deformation process is not known.

The assumption of the initial zero-g system equilibrium condition shown in Fig. 1a, although discussed briefly in the Introduction, needs further clarification. The liquid, being a single mass or glob, is reasonable since liquid slosh (and/or splash) and thermal energy effects are not considered. (The single liquid glob was, of course, the initial zero-g condition in the NASA drop-test results used for correlation with analytical results).

The following is presented to support the added assumption that a thin liquid layer (a few molecules thick) covers the inner-wall surfaces before entering zero-g. The force balance for the three-phase system, Fig. 3, is the Dupre equation

$$\sigma_{sv} - \sigma_{sl} = \sigma_{lv} \cos\theta \tag{1}$$

For a totally wetting liquid, $\cos\theta$ is unity and the Dupre equation is simply

$$\sigma_{sv} - \sigma_{sl} = \sigma_{lv} \tag{2}$$

Equations (1) and (2) are valid at equilibrium only; i.e.,

point P in Fig. 3 is stationary. Before equilibrium is reached, the following equation can be written for a totally wetting liquid:

$$\sigma_{sv} - \sigma_{sl} = \sigma_{lv} + K \tag{3}$$

In Eq. (3), K is Harkins' spreading coefficient.[6] A wetting liquid has a positive K; i.e., adhesion ($\sigma_{sv} - \sigma_{sl}$) is greater than cohesion (σ_{lv}). Spreading will not occur when K is negative. A totally wetting liquid will spread a liquid film over the internal surface of its container. This spreading phenomenon is influenced by gravity only in its thickness. Spreading coefficients determined experimentally for n-heptane on various metals are presented in Ref. 7.

This liquid-spreading phenomenon reduces the number of interfaces for a liquid-vapor-solid system to liquid/solid and liquid/vapor. Of the two, only the liquid/vapor interface can be reduced in zero-g.

Analysis

Because of assumption 6, total free surface energy for a totally wetting liquid is simply

$$\text{SE} = (\sigma A)_{lv} \tag{4}$$

Free surface energy will tend toward a minimum in zero-g. If surface tension is constant, this minimum energy will result when the liquid/vapor interfacial area is a minimum.

The IBM 1620 integration was made for thirty equal increments of Y_n, $(\Delta Y)_n$ in Fig. 2. Incremental free surface energy is shown in Fig. 2. The initial zero-g, or gravity-dominated, free surface energy SE_0 is from Fig. 2a:

$$\text{SE}_0 = \pi\sigma(a^2 + 2rc) \tag{5}$$

During the initial deformation shown in Fig. 2b, free surface energy is

$$\text{SE}_1 = 2\pi\sigma[s(e + f) + r(c - e)] \tag{6}$$

Therefore, the initial incremental surface energy ($n = 1$) is simply

$$\Delta\text{SE}_1 = \text{SE}_0 - \text{SE}_1 \qquad (n = 1) \tag{7}$$

Incremental liquid mass, Fig. 2, is

$$\Delta m_1 = \rho_l[(V_l)_1 - (V_l)_0] \qquad (n = 1) \tag{8}$$

The elapsed time for the liquid deformation, shown in Fig. 2, can be calculated by equating incremental surface energy to incremental kinetic energy. Incremental kinetic energy is

$$\Delta\text{KE}_1 = (\Delta m_1/2g_c)\,(\Delta Y/\Delta\tau)_1^2 \qquad (n = 1) \tag{9}$$

or incremental deformation time then becomes

$$\Delta\tau_1 = \frac{(\Delta Y)_1}{(2g_c)^{1/2}}\left(\frac{\Delta_m}{\Delta SE}\right)_1^{1/2} \qquad (n = 1) \tag{10}$$

Total deformation time τ is then the summation of the incremental times

$$\tau = \sum_{n=1}^{n=30} \Delta\tau_n \tag{11}$$

The IBM integration was made for a sphere of 1-ft-radius and for a liquid kinematic surface tension β of 10^{-3} ft^3/sec^2. The liquid can be either ethyl alcohol or hydrogen since each has a β value of 10^{-3} ft^3/sec^2. The computed results are presented as a dimensionless parameter τ_p for various liquid-to-container volume ratios ξ_p in Fig. 4.

Correlation with NASA Drop-Test Data

Assumption 1 states that the change in free surface energy is the change in kinetic energy of the liquid, or

$$\Delta\text{SE} = \Delta\text{KE} \tag{12}$$

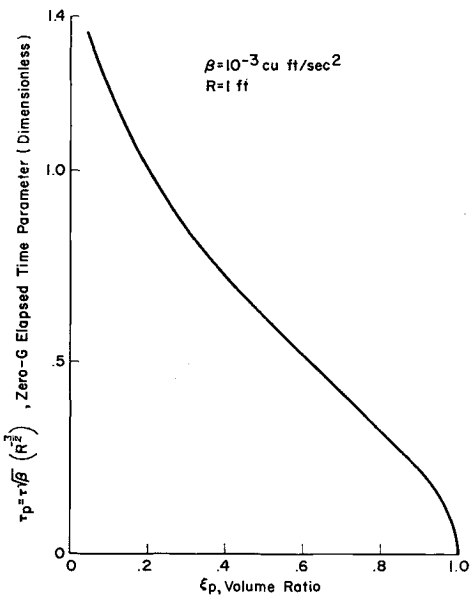

Fig. 4 Dimensionless time parameter vs liquid-to-container volume ratios.

$$\text{SE} \approx \sigma R^2 \tag{13}$$

$$\text{KE} = mv^2/2 \tag{14}$$

If it is assumed that $m \approx \rho R^3$ and $Y = R$, and since

$$v = Y/\tau \tag{15}$$

then

$$\text{KE} \approx \rho R^5/2\tau^2 \tag{16}$$

Now equating SE to KE, it is seen that

$$\tau \approx R^{3/2}\,(1/\beta)^{1/2} \tag{17}$$

The following relationship then can be used to approximate different liquid system deformation times:

$$\tau_a \approx \tau_b\,(R_a/R_b)^{3/2}(\beta_b/\beta_a)^{1/2} \qquad (\xi_a = \xi_b) \tag{18}$$

Subscripts a and b refer to the two different systems.

Now, with reference to Fig. 4, Eq. (18) can be written for any spherical tank radius R and for any kinematic surface tension β as

$$\tau \approx \tau_p R^{3/2}\beta^{-1/2} \qquad (\xi = \xi_p) \tag{19}$$

Results calculated from Eq. (19) were compared to the NASA data. The comparison suggested modification of the equation by a coefficient H:

$$\tau = H\tau_p R^{3/2}\beta^{-1/2} \qquad (\xi = \xi_p) \tag{20}$$

where

$$H = \frac{1}{0.86 - (R_c/R)} \qquad (R > 1.16\,R_c) \tag{21}$$

Correlation between calculated zero-g deformation times from Eq. (20) and the NASA data is presented in Fig. 5. Agreement is relatively good.

The dimensionless coefficient H is presented as a function of R in Fig. 6. H decreases as tank radius increases up to approximately a radius of 1 ft; at larger R values, the value of H approaches a constant equal to 1.16. It should be noted that Eq. (21) is limited to tank radii greater than 1.16 cm.

The assumption that only the displaced liquid, Fig. 2b, is accelerated during deformation probably explains why the correlation coefficient is greater than unity since undoubtedly more liquid is affected.

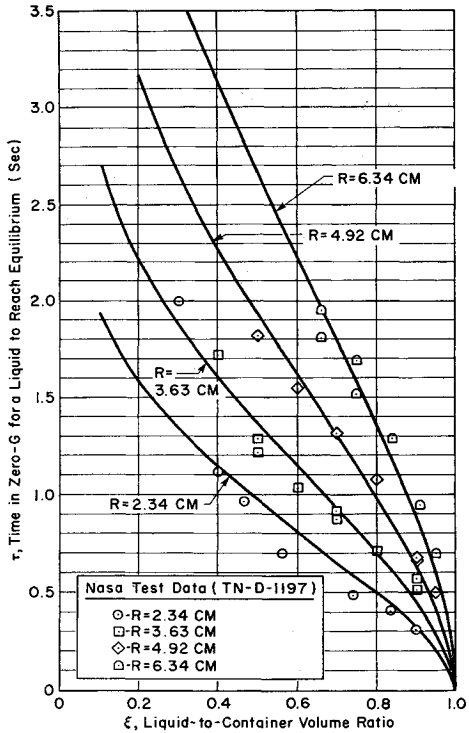

Fig. 5 Correlation of analytical zero-g deformation rates with NASA drop-test data, ethyl alcohol.

The author believes that viscous energy, neglected in this analysis, explains the variation in H at the smaller container sizes ($R < 1.0$ ft) where liquid shear area becomes significant. This effect is evident in Fig. 6; deformation time increases greatly as tank radius decreases from about 1 ft.

Because of viscous energy, H also must be a function of ξ, particularly at low liquid-to-container volume ratios, i.e., when the ratio of ullage volume-to-container volume approaches unity. This phenomenon could not be determined from the NASA data since, except for one datum point, experimental results are limited to an ξ greater than 0.4. More quantitative data at lower ξ values are needed.

Conclusions

Equation (20), which includes the dimensionless time parameter τ_p of Fig. 4, is offered as a method to estimate

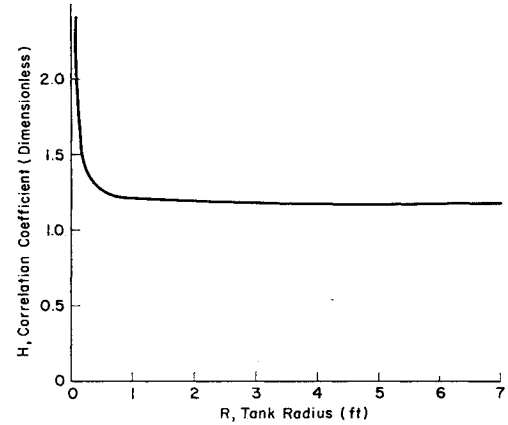

Fig. 6 Correlation coefficient vs tank radii.

zero-g liquid deformation rates for totally wetting liquids in different sized spherical containers with the limitations 1) tank radii greater than 1.16 cm and 2) liquid-to-container volume ratios of 0.4 or more.

The analysis is limited to a spherical container and a totally wetting liquid; however, the method is applicable to any liquid in any tank geometry.

References

[1] Radcliffe, W. F. and Transue, J. R., "Problems associated with multiple engine starts in space craft," ARS J. **31**, 1408–1412 (1961).

[2] Clodfelter, R. G. and Lewis, R. C., "Fluid studies in a zero-gravity environment," Aeronautical Systems Div. TN 61-48 (June 1961).

[3] Unterberg, W. and Congelliere, J., "Zero-gravity problems in space powerplants," ARS J. **32**, 862–872 (1962).

[4] Reynolds, W. C., "Hydrodynamic considerations for the design of systems for very low gravity environments," Stanford Univ. Rept. LG-1, Dept. of Mechanical Engineering, Stanford, Calif. (September 1961).

[5] Petrash, D. A., Zappa, R. F., and Otto, E. W., "Experimental study of the effects of weightlessness on the configuration of mercury and alcohol in spherical tanks," NASA TN-D-1197 (April 1962).

[6] Harkins, W. D., *The Physical Chemistry of Surface Films* (Reinhold Publishing Corp., New York, 1952), Chap. I, pp. 1–83.

[7] Harkins, W. D. and Loeser, E. H., "Surface of solids XIX. Molecular interaction between metals and hydrocarbons," J. Chem. Phys. **18**, 556–560 (1950).